Microvascular Changes in Peripapillary and Optic Nerve Head Tissues After Trabeculectomy in Primary Open-Angle Glaucoma

Ji-Ah Kim,[1] Tae-Woo Kim,[1] Eun Ji Lee,[1] Michaël J. A. Girard,[2,3] and Jean Martial Mari[4]

[1]Department of Ophthalmology, Seoul National University College of Medicine, Seoul National University Bundang Hospital, Seongnam, Korea
[2]Department of Biomedical Engineering, National University of Singapore, Singapore
[3]Singapore Eye Research Institute, Singapore National Eye Centre, Singapore
[4]GePaSud, Université de la Polynésie Française, Tahiti, French Polynesia

Correspondence: Eun Ji Lee, Department of Ophthalmology, Seoul National University Bundang Hospital, Seoul National University College of Medicine, 82, Gumi-ro, 173 Beongil, Bundang-gu, Seongnam, Gyeonggi-do 463-707, Korea; opticdisc@gmail.com.

Submitted: June 13, 2018
Accepted: August 16, 2018

Citation: Kim J-A, Kim T-W, Lee EJ, Girard MJA, Mari JM. Microvascular changes in peripapillary and optic nerve head tissues after trabeculectomy in primary open-angle glaucoma. *Invest Ophthalmol Vis Sci.* 2018;59:4614–4621. https://doi.org/10.1167/iovs.18-25038

Purpose. To determine microvasculature changes in the deep optic nerve head (ONH) and peripapillary tissues after trabeculectomy, and to correlate these with changes in the lamina cribrosa (LC) curvature.

Methods. Fifty-six eyes with primary open-angle glaucoma that underwent trabeculectomy were included. The optic nerve and peripapillary microvasculature were evaluated in en face images obtained using optical coherence tomography (OCT) angiography (OCTA) before and 3 months after trabeculectomy. The OCTA-derived vessel density (VD) was calculated in each layer segmented into the prelaminar tissue (PLT), LC, peripapillary retina (PR), and peripapillary choroid (PPC). Swept-source OCT volume scanning of ONH was performed on the same day as OCTA to examine the change in LC curvature quantified as the LC curve index (LCCI).

Results. At 3 months postoperative, the IOP and LCCI had significantly decreased (both $P < 0.001$). OCTA images revealed a significant increase in VD in the LC ($P = 0.006$), but not in the PLT, PR, or PPC. Twenty-six eyes showed both significant LCCI decrease and VD increase based on 95% Bland-Altman limits of agreement. The VD increase in the LC was significantly associated with larger percentage reductions in IOP ($P = 0.040$) and LCCI ($P < 0.001$) in the univariate analysis. Multivariate analysis revealed that only the LCCI reduction was a significant factor affecting the VD increase in the LC.

Conclusions. A significant increase in VD was observed at the level of the LC after trabeculectomy. The VD increase was more strongly associated with the reduction in the LC curvature than with the reduction of IOP.

Keywords: lamina cribrosa, intraocular pressure, blood flow, trabeculectomy

An elevated intraocular pressure (IOP) is the most important factor contributing to glaucomatous optic nerve damage.[1–4] Mechanical compression and deformation of the lamina cribrosa (LC) associated with IOP elevation is considered to induce axonal injury in glaucoma, by causing kinking and pinching of the retinal ganglion cell (RGC) axons passing through the laminar pores that promote or initiate the blockade of axonal flow.[5–7] It has been shown recently that the degree of LC deformation as measured by the LC depth[8] or LC curvature[9] could be reversed after surgically reducing the IOP. The reversal of LC deformation was associated with a slower rate of glaucomatous thinning of the retinal nerve fiber layer (RNFL),[10] suggesting that the LC reversal may relieve the mechanical stress being imposed on the RGC axons.

IOP-related mechanical stress within the LC can also induce an ischemic insult on the RGC axons.[11] From a biomechanical perspective, an elevated IOP can deform the capillary-containing laminar beams, thereby reducing the blood supply to the laminar segments of the axons.[11] Based on this concept, the reversal of LC deformation with IOP lowering may relieve the compression of the laminar capillaries and thereby enhance the blood supply to the axons.

Optical coherence tomography (OCT) angiography (OCTA) enables noninvasive imaging of the microvasculature in ocular tissues in segmented layers. Studies using OCTA found that the peripapillary retina (PR) microvasculature improved after IOP lowering in glaucomatous eyes[12,13]; however, it remains to be determined whether IOP-lowering treatment also affects the microvasculature in the deep optic nerve head (ONH) and in peripapillary tissues such as the LC or the choroid.

The present study aimed to determine microvasculature changes within the deep ONH and peripapillary tissues after performing surgical IOP lowering in primary open-angle glaucoma (POAG), and to correlate the microvascular changes with the magnitude of the LC-curvature reversal. To achieve this aim, the vessel density (VD) was evaluated separately in the segmented layers of the prelaminar tissue (PLT), LC, PR, and peripapillary choroid (PPC) using en face images obtained by OCTA.

Methods

This study involved POAG patients who were enrolled in the Investigating Glaucoma Progression Study (IGPS), an ongoing prospective study of glaucoma patients at the Glaucoma Clinic of Seoul National University Bundang Hospital. All subjects provided written informed consent to participate. The study protocol was approved by the Institutional Review Board of Seoul National University Bundang Hospital and followed the tenets of the Declaration of Helsinki.

Participants

All participants underwent comprehensive ophthalmic examinations, which included assessments of best-corrected visual acuity (BCVA), Goldmann applanation tonometry, a refraction test, slit-lamp biomicroscopy, gonioscopy, stereo disc photography, red-free fundus photography (EOS D60 digital camera; Canon, Utsunomiyashi, Tochigiken, Japan), central corneal thickness measurement (Orbscan II; Bausch & Lomb Surgical, Rochester, NY, USA), and axial length measurement (IOLMaster version 5; Carl Zeiss Meditec, Dublin, CA, USA). Peripapillary RNFL thickness was measured by spectral-domain OCT (Spectralis; Heidelberg Engineering, Heidelberg, Germany). Other ophthalmic examinations included standard automated perimetry (Humphrey Field Analyzer II 750, 24-2 Swedish interactive threshold algorithm; Carl Zeiss Meditec) and swept-source OCT scanning of the ONH and OCTA (DRI OCT Triton; Topcon, Tokyo, Japan). Clinical history was also taken from participants, including demographic characteristics and the presence of cold extremities, migraine, and other systemic conditions. Systolic and diastolic blood pressures (BPs) were measured using a digital automatic BP monitor (Omron HEM-770A; Omron Matsusaka Co., Ltd., Matsusaka, Japan). Mean arterial pressure (MAP) was calculated using the expression MAP = diastolic BP + 1/3 (systolic BP − diastolic BP), and mean ocular perfusion pressure (MOPP) was calculated using the equation MOPP = 2/3 (MAP − IOP) at the time of OCTA.

POAG was defined as the presence of an open iridocorneal angle, signs of glaucomatous optic nerve damage (i.e., neuroretinal rim thinning, notching, or a RNFL defect), and a glaucomatous visual field (VF) defect. A glaucomatous VF defect was defined as a defect conforming with one or more of the following criteria: (1) outside normal limits on a glaucoma hemifield test, (2) three abnormal points with a <5% probability of being normal and one abnormal point with a <1% probability by pattern deviation, or (3) a pattern standard deviation of probability <5% confirmed on two consecutive reliable tests (fixation loss rate of ≤20% and false-positive and false-negative error rates of ≤25%).

The exclusion criteria were eyes with a BCVA worse than 20/40, a spherical equivalent of <−8.0 diopters (D) or >+3.0 D, a cylinder correction of <−3.0 D or >+3.0 D, a history of intraocular surgery with the exception of uneventful cataract surgery, and retinal (e.g., diabetic retinopathy, retinal vessel occlusion, or retinoschisis) or neurological diseases (e.g., pituitary tumor).

Those patients included in the IGPS who underwent trabeculectomy and for whom pre- and postoperative OCTA results were available were included in the present study. Indications for trabeculectomy were IOP deemed to be associated with a high risk of progression, or glaucomatous progression of the VF or optic disc despite taking the maximum tolerated medications. All ocular hypotensive medications were continued up to the time of surgery. Eyes with signs of hypotony, maculopathy, or disc edema after surgery were excluded.

The microvasculature in the deep ONH and peripapillary area was evaluated using OCTA at 1 day before surgery and 3 months postoperatively. Swept-source OCT scanning of the ONH and measurement of IOP were performed at the time of OCTA.

Measurement of VD Using OCTA

The optic nerve and peripapillary area were imaged using a commercially available swept-source OCTA device (DRI OCT Triton; Topcon), with a central wavelength of 1050 nm, an acquisition speed of 100,000 A-scans per second, and axial and transversal resolutions of 7 and 20 μm in the tissue, respectively. This instrument uses an active eye tracker that follows the eye movement, detects blinking, and adjusts the scan position accordingly, thereby reducing motion artifacts during the acquisition of OCTA images. Scans were taken from 4.5×4.5-mm cubes, with each cube consisting of 320 clusters of four repeated B-scans centered on the optic disc. En face projections of the volumetric scans made it possible to visualize the structural and vascular details within each segmented layer. Each included B-scan image had an image quality score of ≥30, in accordance with the manufacturer's recommendation. When the quality of the OCTA images was poor (e.g., due to blurring) or when the vascular signal was blocked by artifacts (e.g., due to blinking or masking[14]), the eye was excluded from the analysis.

The DRI OCT Triton device allows the microvasculature in regions of interest (ROIs) to be evaluated in a customized manner. Using manual segmentation, en face OCTA images were first produced in the segmented layers of the PLT (from the internal limiting membrane to the anterior LC border) and PR (from the internal limiting membrane to the retinal pigment epithelium), and then of the LC (from the anterior to posterior borders of the LC) and PPC (below the RPE including the choroid and anterior sclera) (Fig. 1A).

The scanned images were extracted from the OCTA instrument and imported into the publicly available ImageJ software (http://imagej.nih.gov/ij/; provided in the public domain by the National Institutes of Health, Bethesda, MD, USA). Because contrast among en face images can differ between those obtained before and after the surgery, which may result in a falsely higher/lower VD, the extracted en face images were binarized according to Niblack's method.[15,16] The idea of Niblack's method is to vary the threshold over the image, based on the local mean, m, and local standard deviation, s, computed in a small neighborhood of each pixel. A threshold for each pixel is computed from $T = m + k*s$, where k is a user-defined parameter and constant getting negative values. The black region was considered as vascular area and its number of pixels was quantified with ImageJ software. Four ROIs were determined based on Bruch's membrane opening (BMO; inner ellipse in Figs. 1D, 1E) and a 750-μm-wide elliptical annulus extending outward from the BMO (outer ellipse in Figs. 1D, 1E). The ROIs encompassed by the inner ellipse were used to assess VDs in the PLT and LC, and those between the inner and outer ellipses were used to assess VDs in the PR and PPC. The VD in each ROI was calculated by dividing the number of pixels in the vascular area by that of the ROI and expressing this as a percentage. The VD was measured on the images obtained preoperatively and 3 months postoperatively.

Measurement of LC Curve Index (LCCI)

The degree of LC deformation was assessed by measuring the LC curvature in the seven locations equidistant across the vertical optic disc diameter using horizontal B-scan images. The

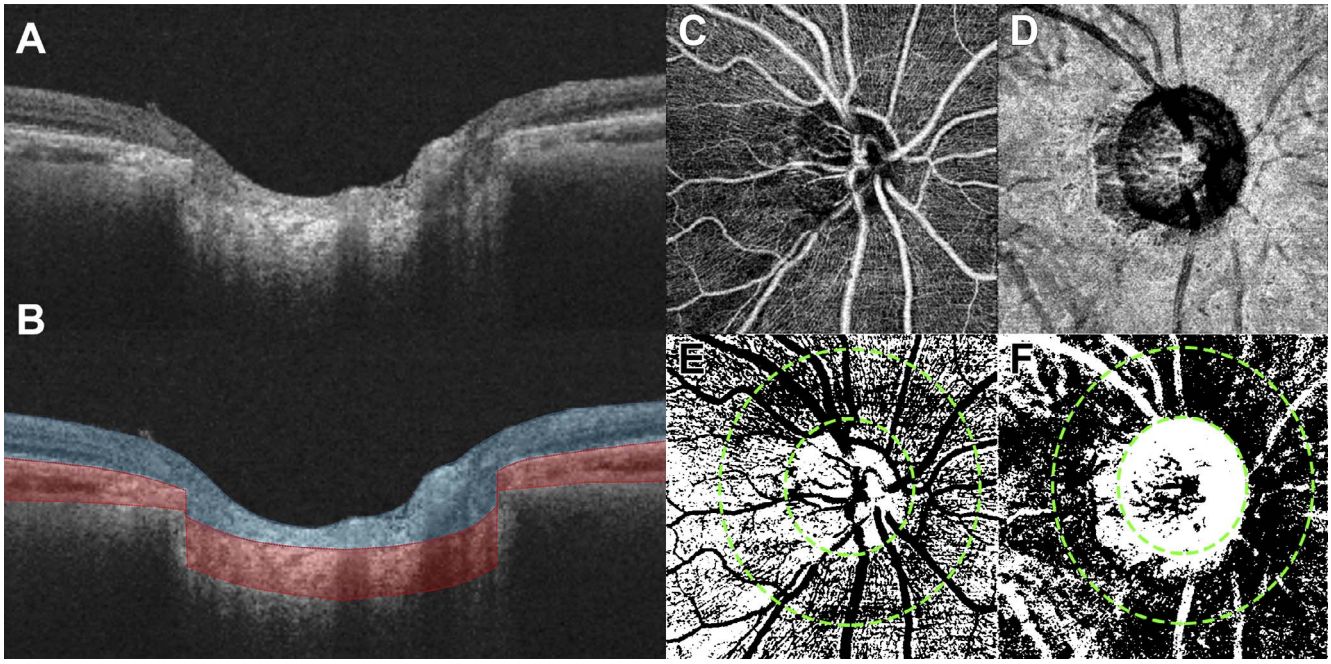

Figure 1. Production of en face OCTA images segmented into the layers of the PLT, LC, PR, and PPC, and determination of the ROIs. (**A**) B-scan image of the ONH. (**B**) Same image as (**A**) indicating the segmented layers of the PLT and PR (*blue area*) and the LC and PPC (*red area*), which produced the en face images shown in (**C**) and (**D**), respectively. (**E**, **F**) Same images as (**C**) and (**D**) after binarization, with the ROIs indicated. *Inner ellipses* and *outer ellipses* were used to measure the vessel densities in the PLT and LC, and in the PR and PPC, respectively.

LC curvature was determined using the LCCI, which was defined as the inflection of a curve representing a section of the LC.[9,17] The LCCI was determined by first measuring the width of BMO (*W*) and then measuring the LC curve depth (LCCD) within the BMO in each B-scan (Fig. 2). The BMO width (*W*) was defined as the distance between the temporal and nasal termination point. Lines were drawn from each Bruch's membrane termination point perpendicular to the BMO reference line, until they met the anterior LC surface. The line connecting the two points on the anterior LC surface was used as the reference line to measure the LCCD, which was defined as the maximum LC depth from the reference line (Fig. 2). The LCCI was then calculated as (LCCD/*W*) × 100. Because the curvature was thereby normalized according to LC width, it describes the shape of the LC independent of the actual size of the ONH. Only the LC within the BMO was considered because the LC was often not clearly visible outside of the BMO. In eyes with LC defects, the LCCI was measured using a presumed anterior LC surface that best fit the curvature of the remaining part of the LC or excluding the area of LC defect.

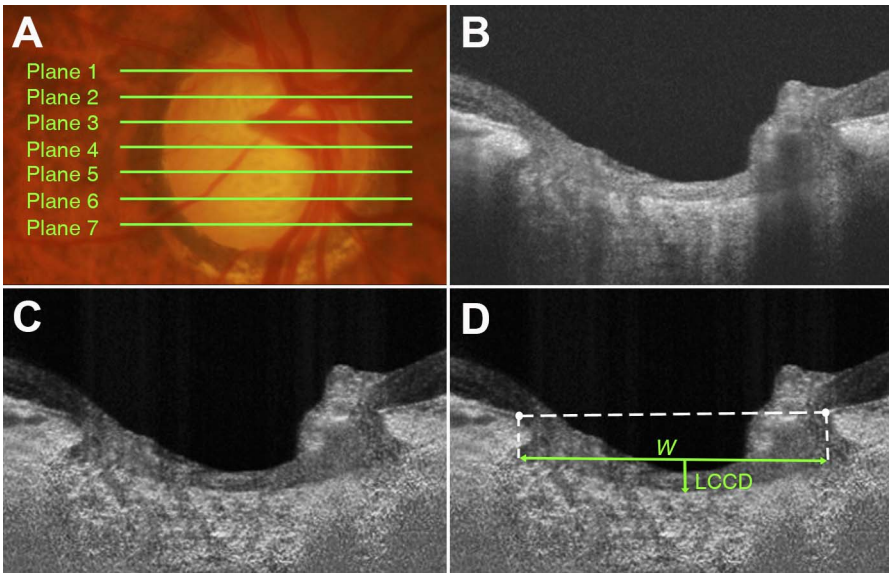

Figure 2. Measurement of the LCCI. (**A**) Disc photograph with seven horizontal *green lines* indicating the locations at which the measurements were performed. (**B**) B-scan image obtained at plane 5 in (**A**). (**C**, **D**) Same images as in (**B**) postprocessed by adaptive compensation. (**D**) The LCCI was measured by dividing the LCCD within the BMO by the BMO width (*W*), and then multiplying by 100.

Table 1. Demographic Characteristics of Participants ($n = 56$)

Variables	Mean ± Standard Deviation
Age, y	55.6 ± 15.9
Male/Female	41/15
Central corneal thickness, μm	549.6 ± 40.9
Axial length, mm	25.02 ± 2.08
Spherical equivalent, D	−2.17 ± 3.14
Global RNFL thickness, μm	65.04 ± 22.42
VF MD, dB	−15.17 ± 9.43
VF PSD, dB	8.09 ± 3.70
Systolic BP, mm Hg	129.6 ± 14.8
Diastolic BP, mm Hg	77.1 ± 10.3
MAP, mm Hg	94.6 ± 11.1
MOPP, mm Hg	47.9 ± 9.5
Self-reported history of hypertension, *n* (%)	14 (25.0)
Self-reported history of diabetes, *n* (%)	10 (17.9)
Glaucoma family history, *n* (%)	4 (7.1)
Cold extremities, *n* (%)	13 (23.2)
Migraine, *n* (%)	5 (8.93)

Values are shown in mean ± SD, unless otherwise specified. MD, mean deviation; PSD, pattern standard deviation.

Before the measurement, the visibility of the peripheral LC was enhanced by postprocessing images by using adaptive compensation.[18,19] Measurement was performed by using a manual caliper tool in the Amira software (version 5.2.2; Visage Imaging, Berlin, Germany) at seven selected B-scan images spaced equidistantly across the vertical optic disc diameter in each eye. The measurements obtained from the seven B-scans were used to calculate the mean LCCI of the eye.

The LCCI was measured on the B-scan images obtained preoperatively and 3 months postoperatively. For the follow-up measurement, the B-scan images were selected to correspond with those that had been selected for the baseline measurements by using the en face images and the low reflective shadow within the LC to confirm the correspondence of the B-scan image series between the two time points.[8–10]

The LCCIs were measured by two experienced observers (JAK and EJL) who were masked to the clinical information. The average of the measurements from each of the two observers was used for analysis.

Data Analysis

The interobserver agreement for measuring the LCCI was evaluated by calculating intraclass correlation coefficients (ICCs). Significant changes of the measured parameters were defined as those exceeding the 95% Bland-Altman limits of agreement. The χ^2 test with linear-by-linear association test was used to examine the association between the changes in the VD and the LCCI. The pre- and postoperative amounts of IOP, LCCI, and VD were compared using the paired *t*-test. Regression analysis was used to investigate the factors associated with the amount of VD change, first with a univariate model and then with a multivariate model that included variables from the univariate model for which $P < 0.10$. Statistical analyses were performed by using the Statistical Package for the Social Sciences software (version 22.0; SPSS, Chicago, IL, USA). Probability values of $P < 0.05$ were considered indicative of statistical significance. Except where stated otherwise, the data are presented as mean ± SD values.

Table 2. Pre- and Postoperative Measurements of IOP, LCCI, VD in the prelaminar tissue, LC, PR, and PPC, and Quality Scores of OCTA Images

	Preoperative	Postoperative	*P*
IOP, mm Hg	23.1 ± 7.5	13.0 ± 4.9	**< 0.001**
LCCI	13.2 ± 2.7	10.8 ± 2.2	**< 0.001**
VD in the prelaminar tissue, %	31.6 ± 9.6	32.6 ± 10.6	0.307
VD in the LC, %	10.2 ± 4.7	11.9 ± 6.0	**0.006**
VD in the PR, %	28.6 ± 7.4	28.2 ± 7.7	0.558
VD in the PPC, %	75.4 ± 10.4	75.7 ± 10.5	0.637
Image quality score	62.5 ± 6.2	61.8 ± 6.9	0.437

Values are shown in mean ± SD. Values with statistical significance are in boldface.

Table 3. Distribution of the Patients Showing Significant Change in the VD in the LC and in the LCCI

	VD of LC				
LCCI	Increase	No Change	Decrease	Total	*P**
Decrease	26	7	3	36	<0.001
No change	3	8	9	20	
Increase	0	0	0	0	
Total	29	15	12	56	

* χ^2 test with linear-by-linear association analysis.

Results

Seventy-seven patients with POAG who underwent trabeculectomy were initially included. Sixteen of them were excluded owing to poor scan image quality, and five of them were excluded owing to signs of hypotony after surgery, leaving a final sample of 56 patients. Table 1 summarizes the clinical characteristics of participants. There was excellent interobserver agreement in measurements of the LCCI (mean ICC = 0.979, 95% confidence interval = 0.970–0.986).

At 3 months postoperatively, the IOP and LCCI had decreased significantly from 23.1 ± 7.5 to 13.0 ± 4.9 mm Hg and from 13.23 ± 2.65 to 10.80 ± 2.20, respectively (Table 2; both $P < 0.001$, paired *t*-test). The VD had increased significantly in the LC at 3 months postoperatively (from 10.21% ± 4.72% to 11.88% ± 6.04%, $P = 0.006$; Table 2). However, there were no statistically significant differences between the pre- and postoperative VDs in the layers of the PLT, PR, and PPC ($P = 0.307$, 0.558, and 0.637, respectively; Table 2).

The significant changes of LCCI and VD in the LC were calculated using test-retest variability based on the 20 image pairs of 20 stable POAG patients that were obtained within a 3-month period. The 95% Bland-Altman limits of agreement between the measurements were −1.63 and 1.43 for the LCCI and −1.39 and 0.94 for the VD in the LC. Based on these values, 36 eyes showed significant decrease in the LCCI, and 29 showed significant increase in the VD. Of these, 26 eyes showed both decreased LCCI and increased VD in the LC. Distribution of eyes showing significant changes in the LCCI and VD in the LC is shown in Table 3. A significant association was documented between increased VD in the LC and decreased LCCI ($P < 0.001$, χ^2 test with linear-by-linear association analysis).

Factors associated with the increase in VD in the LC were determined using linear regression analysis. In the univariate analysis, larger percentage reductions in IOP ($P = 0.040$) and LCCI ($P < 0.001$) were significantly associated with the increase in VD in the LC (Table 4; Fig. 3). Multivariate analyses were performed in two ways to avoid multicollinearity between the changes in IOP and LCCI. The analyses revealed

Table 4. Factors Associated With the Increase of VD in the LC at Postoperative Month 3

	Univariate		Multivariate 1*		Multivariate 2*	
Variables	β (95% CI)	*P*	β (95% CI)	*P*	β (95% CI)	*P*
Age, per 1 y older	−0.039 (−0.114 to 0.035)	0.293				
Female sex	1.557 (−1.083 to 4.197)	0.242				
CCT, per 1 μm larger	−0.013 (−0.042 to 0.016)	0.383				
AXL, per 1 mm larger	0.027 (−0.545 to 0.600)	0.924				
Global RNFL thickness, per 1 μm larger	0.028 (−0.024 to 0.081)	0.285				
VF MD, per 1 dB higher	−0.022 (−0.141 to 0.097)	0.711				
Baseline IOP, per 1 mm Hg higher	0.085 (−0.073 to 0.243)	0.287				
% IOP reduction, per 1% larger	**0.060 (0.003 to 0.116)**	**0.040**	0.055 (−0.001 to 0.111)	0.055		
Baseline LCCI, per 1 unit larger	0.281 (−0.163 to 0.726)	0.210				
% LCCI reversal, per 1% larger	**0.199 (0.107 to 0.292)**	**<0.001**			**0.188 (0.095 to 0.281)**	**<0.001**
Baseline VD in the LC, per 1% larger	−0.109 (−0.361 to 0.142)	0.388				
SBP, per 1 mm Hg higher	−0.038 (−0.118 to 0.042)	0.346				
DBP, per 1 mm Hg higher	−0.039 (−0.155 to 0.076)	0.498				
MAP, per 1 mm Hg higher	−0.045 (−0.152 to 0.062)	0.402				
MOPP, per 1 mm Hg higher	−0.076 (−0.199 to 0.048)	0.225				
Self-reported hypertension	−0.540 (−3.271 to 2.191)	0.693				
Self-reported diabetes	−0.942 (−4.023 to 2.139)	0.542				
Family history of glaucoma	−0.260 (−4.857 to 4.338)	0.910				
Cold extremities	2.028 (−0.722 to 4.777)	0.145				
Migraine	3.730 (−0.297 to 7.756)	0.069	3.341 (−0.605 to 7.287)	0.095	2.372 (−1.247 to 5.991)	0.194
Image quality score	0.106 (−0.072 to 0.283)	0.238				

Values with statistical significance are in boldface. AXL, axial length; CCT, central corneal thickness; DBP, diastolic blood pressure; SBP, systolic blood pressure.

* Only variables with $P < 0.1$ on univariate analysis were included in the multivariate model.

that only the percentage LCCI reduction was a significant factor affecting the increased VD in the LC ($P < 0.001$), whereas the percentage IOP reduction was marginally significant ($P = 0.055$). Figure 4 illustrates a case in which the LCCI reduction after trabeculectomy was associated with an increase in VD in the LC.

Discussion

The present study demonstrated that VD increased at the level of the LC after trabeculectomy using OCTA. The magnitude of the VD increase in the LC was positively associated with the magnitude of the reduction in the LCCI. To our knowledge, this is the first report of changes in VD in the deep optic nerve and peripapillary tissues in human glaucomatous eyes after glaucoma surgery. Although an elevated IOP has been considered the most important factor contributing to glaucomatous optic nerve damage,[1–4] factors other than IOP have also been implicated in the progression of glaucoma.[20] The present study may provide a key to understand the link between perfusion and mechanical deformation of the ONH in the context of incisional glaucoma surgery.

It has been shown that reducing the IOP increases the ocular perfusion pressure, which enhances ocular blood flow. There are previous reports of trabeculectomy improving the retrobulbar blood flow based on color Doppler imaging,[21–23] the pulsatile ocular blood flow based on the fundus pulsation

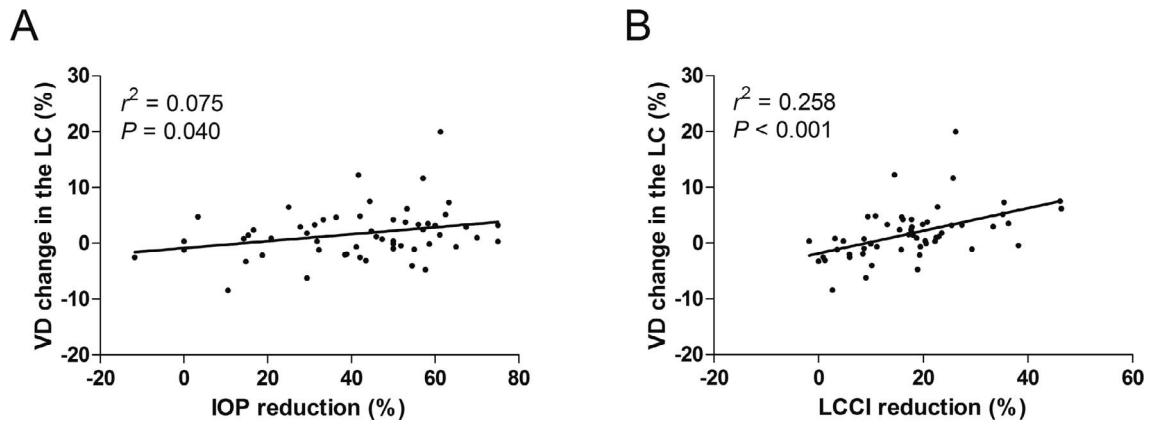

Figure 3. Scatterplots showing the relationships of the percentage IOP reduction (**A**) and the percentage LCCI reduction (**B**) with the VD change in the LC.

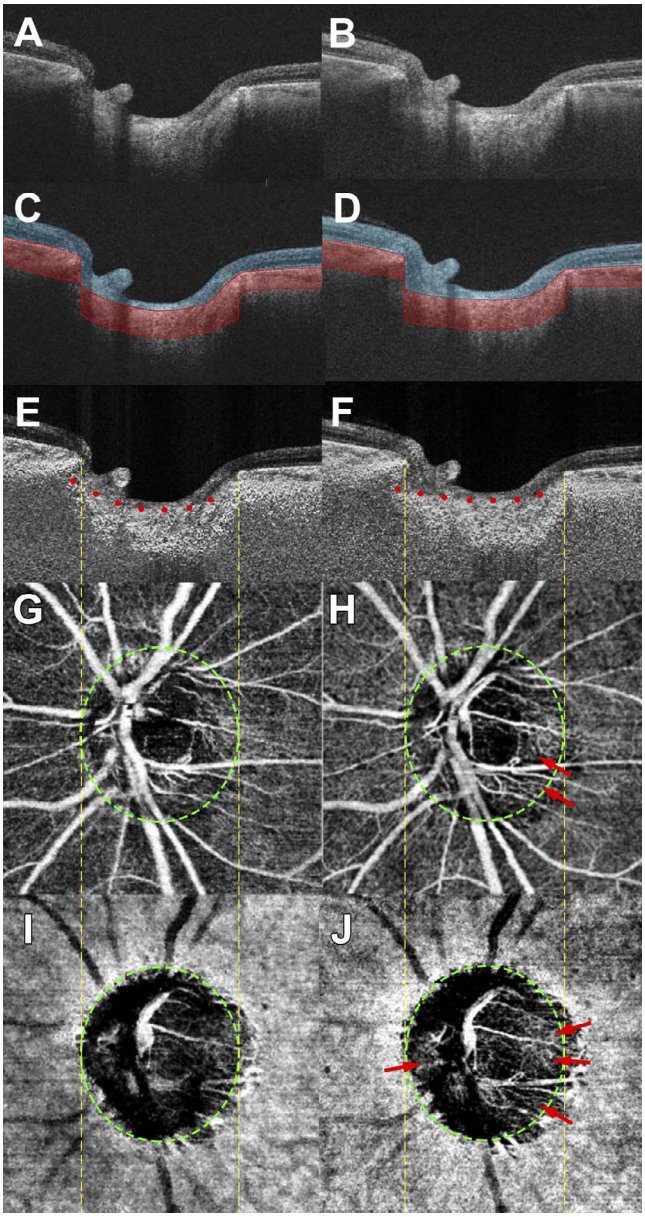

Figure 4. A glaucomatous eye that underwent trabeculectomy, where reduction of the LC curvature was associated with an increased VD in the LC. Images in the *left* and *right* columns were obtained at 1 day preoperatively and at 3 months postoperatively, respectively. (**A**, **B**) B-scan images of the optic nerve obtained in the central portion (plane 4 in Fig. 2A). (**C, D**) Same image as (**A, B**) indicating the segmented layers of the prelaminar tissue and PR (*blue area*), and the LC and PPC (*red area*). (**E, F**) Same images as (**A, B**) postprocessed by adaptive compensation show the flattened LC curvature after surgery (*red dots*). (**G–J**) En-face OCTA images produced in the segmented layers of PLT and PR (**G**, **H**) and LC and PPC (**I**, **J**). Note the subtle but noticeable increase in VD in the prelaminar tissue (**H**, *arrows*), and the significant increase in VD in the LC (**J**, *arrows*) after surgery. *Yellow dashed lines* and *green dashed ellipses* indicate BMO.

amplitude,[22,24,25] and the ONH blood flow based on scanning laser Doppler flowmetry.[24] Comparable to these findings, recent studies using OCTA have demonstrated an increased VD in the PR after medical[13] or surgical[12] IOP lowering.

The present study examined the change in VD after trabeculectomy separately in the superficial and deep layers of peripapillary and ONH tissues, and showed that the VD increased in the LC, but not in the PLT, PR, or PPC. These findings are inconsistent with previous studies showing an improved microvasculature in the PR.[12,13] This discrepancy may be attributable to the lower preoperative IOP (23.1 mm Hg) and smaller IOP reduction (10.1 mm Hg, 43.7%) in the present study. Hollo[13] reported that VD in the PR increased after medical IOP lowering. The patients in their study had a baseline IOP higher than 35 mm Hg, and the magnitude of the IOP reduction was at least 50% from the baseline IOP. The preoperative IOP in the study of Shin et al.[12] was 26.3 mm Hg, which is higher than that in our study. That previous study found that the maximum reduction in IOP was lower in eyes not showing an improved microvasculature (11.0 mm Hg) than in those showing an improved microvasculature (19.7 mm Hg). The lower preoperative IOP and smaller IOP reduction of our patients might have resulted in the increase in the MOPP, being too small to detect a significant change in VD in the PR. Another possible reason for the inconsistent finding would be the different methodology used to quantify retinal vasculature.

In the current study, the increase in VD in the LC was associated with the magnitude of the LCCI reduction. Shin et al.[12] found a significant correlation between the improvement in the retinal microvasculature and the LC depth reduction after IOP lowering. This is in part in disagreement with our study, given that both LC depth and LCCI are parameters representing LC deformation. The principal arterial blood supply to the PLT and LC is via direct branches of the short posterior ciliary arteries (SPCA) and via vessels originating from the arterial circle of Zinn-Haller.[26] On the other hand, the retinal capillaries are supplied solely by the central artery of the retina except for sparse cilioretinal arteries.[27] Therefore, the decompression of capillaries within the LC might not be directly associated with an improved retinal microvasculature. Further, it is less likely that the reduction of LC depth relieved the compression of the large central retinal artery within the LC to result in enhancement of the retinal blood flow. The reduction of the LC depth and increased retinal VD observed by Shin et al.[12] might have been observed concurrently following a large reduction in IOP. We suggest that the increased VD in the LC found in our study reflects relief of the compression of the laminar capillaries associated with reduced the LC strain after IOP lowering.

The magnitude of the IOP lowering was only marginally associated with the magnitude of the VD increase in the LC. This may indicate that IOP reduction itself is not the crucial factor for reducing the LC strain. Our group previously found that reversal of the LC depth was not observed in 41% of eyes after IOP-lowering treatment.[28] The individual susceptibility to IOP-related stresses and strains is affected by various biomechanical factors involving the ONH,[11] and so reducing IOP might not necessarily reverse deformation of the LC. The significant influence of LCCI reduction on the VD increase (and not that of IOP reduction) in our study may indicate that microvascular changes after trabeculectomy are better represented by changes in LCCI rather than IOP itself. On the other hand, it is also possible that the relatively small IOP reduction in our study resulted in the lack of a significant influence of the IOP reduction on the VD increase. Longitudinal studies investigating the relationship between the change in LC structural and perfusion variables and glaucoma progression is anticipated in the near future. If such relationship is confirmed, imaging of the LC vasculature could serve as a tool to assess perfusion of the ONH, not only in glaucomatous eyes with high IOP requiring surgery, but also in those with normal IOP. It is possible that enhancement of perfusion to LC pharmacologically or by other means provides benefit to glaucoma patients independently of IOP.

The VD in the PLT and PPC did not change significantly in the current study. The PLT and PPC are supplied by SPCA, and thus share a common arterial supply with the LC. The presence of a significant VD increase only in the LC and not in the PLT or PPC may indicate that the microvasculature improvement primarily occurs at the level of the LC, and is independent of a change in the blood flow in the choroid or SPCA. Previous studies found that the choroidal perfusion was sustained until the IOP exceeded 50 mm Hg.[29,30] The highest and mean IOPs in our subjects were 46 and 23 mm Hg, respectively, and so it is reasonable to expect that the VD in the choroid would not change. Again, the decreased LC strain as indicated by the LCCI reduction may have contributed to relieving the compression of the capillaries in the LC, resulting in the VD increase in the LC. Whether the increased VD in the LC indicates better perfusion to the ONH axons remains to be determined.

We used LCCI rather than the LC depth as the parameter relevant to LC strain in this study. Although the LC depth has been used in both experimental and clinical studies,[31–33] it is measured from the level of BMO and so includes the choroidal thickness, which is known to vary between individuals.[34] Moreover, it is known that the choroidal thickness increases after trabeculectomy.[35] Therefore, using the LC depth as measured from BMO may result in biased assessments of LC strain. In contrast, the LCCI is not affected by the choroidal thickness, and we recently showed that it was easier to discriminate between healthy and glaucomatous eyes when using the LCCI rather than the LC depth,[17] suggesting that the LCCI is better for characterizing LC deformation in glaucomatous eyes.

It is theoretically possible that OCTA cannot detect vertically moving flow as it can detect horizontally moving flow. Given this, it is possible that the change in the LCCI influenced the visibility of the LC microvasculature. However, most of the capillaries in the laminar trabeculae run horizontally with capillary interconnections between various LC levels running vertically.[36] In addition, it has been suggested that OCTA can detect both transverse and axial flow with similar sensitivities.[37–41] Therefore, the influence of LCCI change on the visibility of VD in the LC might have been negligible.

The findings of this study should be considered in the light of some limitations. First, the layers within each ROI were segmented manually to produce en face OCTA images. This was necessary because the current version of the DRI OCT Triton device cannot segment the anterior and posterior borders of the LC automatically. However, all of the 320 B-scan images obtained in a single OCTA examination were carefully examined to avoid segmentation errors. Second, the OCTA modality used in the present study has limitations in the analysis of segmented layers, especially the deeper layers, because artifacts due to vascular shadowing or projection onto the underlying tissues are unavoidable.[42,43] In addition, the VD measured using OCTA may not completely represent anatomical VD. However, our study evaluated the change in VD in the same ONH areas in each subject, which should have minimized the effect of any limitation in the microvascular visibility on our main results. Moreover, considering that the VD in the PLT did not significantly increase after trabeculectomy in our subjects, the influence of the artifacts might not have affected the conclusion. Third, although paired *t*-test showed that VD increase in the LC was statistically significant, the absolute amount of the VD increase was of small degree; however, the mean change exceeded the upper limit of test-retest variability (0.940), confirming that the observed change was indeed of significant degree. Fourth, the signal of the microvessels in the binarized OCTA images does not resemble anatomical vasculature, and so the VD measured in this study may not represent actual VD. However, en face OCTA images were grayscale, thus binarization was necessary to adjust interimage contrast. Last, OCTA images were obtained at two time points, preoperatively and at 3 months postoperatively, and patients were observed only for up to 3 months after trabeculectomy. However, our group previously found that the reduction of the LC depth after trabeculectomy occurred mainly before 3 months postoperatively.[8] We therefore believe that evaluating the LC change at postoperative month 3 should be sufficient to evaluate the resilience of the LC.

In conclusion, OCTA revealed a significant increase in VD at the level of the LC after trabeculectomy. The magnitude of the VD increase was positively associated with the magnitude of the LCCI reduction. This finding suggests that the reduction of LCCI induced by IOP lowering relieves the compression of the capillary within the LC and thus potentially enhances blood flow to the ONH axons. Future studies should determine whether the increased VD in the LC plays a role in preventing glaucoma progression.

Acknowledgments

The authors thank Hyunjoong Kim, PhD, Department of Applied Statistics, Yonsei University, Seoul, Korea, for providing advice about the statistical analysis.

Supported by Seoul National University Bundang Hospital Research Fund (no. 02-2017-037).

Disclosure: **J.-A. Kim**, None; **T.-W. Kim**, None; **E.J. Lee**, None; **M.J.A. Girard**, None; **J.M. Mari**, None

References

1. Gordon MO, Beiser JA, Brandt JD, et al. The Ocular Hypertension Treatment Study: baseline factors that predict the onset of primary open-angle glaucoma. *Arch Ophthalmol*. 2002;120:714–720; discussion 829–730.
2. Kass MA, Heuer DK, Higginbotham EJ, et al. The Ocular Hypertension Treatment Study: a randomized trial determines that topical ocular hypotensive medication delays or prevents the onset of primary open-angle glaucoma. *Arch Ophthalmol*. 2002;120:701–713; discussion 829–730.
3. The AGIS Investigators. The Advanced Glaucoma Intervention Study (AGIS): 7. The relationship between control of intraocular pressure and visual field deterioration. *Am J Ophthalmol*. 2000;130:429–440.
4. Leske MC, Heijl A, Hussein M, et al. Factors for glaucoma progression and the effect of treatment: the early manifest glaucoma trial. *Arch Ophthalmol*. 2003;121:48–56.
5. Quigley H, Anderson DR. The dynamics and location of axonal transport blockade by acute intraocular pressure elevation in primate optic nerve. *Invest Ophthalmol*. 1976; 15:606–616.
6. Quigley HA, Addicks EM, Green WR, Maumenee AE. Optic nerve damage in human glaucoma. II. The site of injury and susceptibility to damage. *Arch Ophthalmol*. 1981;99:635–649.
7. Gaasterland D, Tanishima T, Kuwabara T. Axoplasmic flow during chronic experimental glaucoma. 1. Light and electron microscopic studies of the monkey optic nervehead during development of glaucomatous cupping. *Invest Ophthalmol Vis Sci*. 1978;17:838–846.
8. Lee EJ, Kim TW, Weinreb RN. Reversal of lamina cribrosa displacement and thickness after trabeculectomy in glaucoma. *Ophthalmology*. 2012;119:1359–1366.
9. Lee SH, Yu DA, Kim TW, Lee EJ, Girard MJ, Mari JM. Reduction of the lamina cribrosa curvature after trabeculectomy in glaucoma. *Invest Ophthalmol Vis Sci*. 2016;57:5006–5014.

10. Lee EJ, Kim TW. Lamina cribrosa reversal after trabeculectomy and the rate of progressive retinal nerve fiber layer thinning. *Ophthalmology*. 2015;122:2234–2242.
11. Burgoyne CF, Downs JC, Bellezza AJ, Suh JK, Hart RT. The optic nerve head as a biomechanical structure: a new paradigm for understanding the role of IOP-related stress and strain in the pathophysiology of glaucomatous optic nerve head damage. *Prog Retin Eye Res*. 2005;24:39–73.
12. Shin JW, Sung KR, Uhm KB, et al. Peripapillary microvascular improvement and lamina cribrosa depth reduction after trabeculectomy in primary open-angle glaucoma. *Invest Ophthalmol Vis Sci*. 2017;58:5993–5999.
13. Hollo G. Influence of large intraocular pressure reduction on peripapillary OCT vessel density in ocular hypertensive and glaucoma eyes. *J Glaucoma*. 2017;26:e7–e10.
14. Ghasemi Falavarjani K, Al-Sheikh M, Akil H, Sadda SR. Image artefacts in swept-source optical coherence tomography angiography. *Br J Ophthalmol*. 2017;101:564–568.
15. Sauvola J, Seppanen T, Haapakoski S, Pietikainen M. Adaptive document binarization. In: *Proceedings of the Fourth International Conference on Document Analysis and Recognition*. Ulm, Germany: IEEE; 1997:147–152.
16. Niblack W. *An Introduction to Digital Image Processing*. Birkeroed, Denmark: Strandberg Publishing Company; 1986.
17. Lee SH, Kim TW, Lee EJ, Girard MJ, Mari JM. Diagnostic power of lamina cribrosa depth and curvature in glaucoma. *Invest Ophthalmol Vis Sci*. 2017;58:755–762.
18. Girard MJ, Strouthidis NG, Ethier CR, Mari JM. Shadow removal and contrast enhancement in optical coherence tomography images of the human optic nerve head. *Invest Ophthalmol Vis Sci*. 2011;52:7738–7748.
19. Mari JM, Strouthidis NG, Park SC, Girard MJ. Enhancement of lamina cribrosa visibility in optical coherence tomography images using adaptive compensation. *Invest Ophthalmol Vis Sci*. 2013;54:2238–2247.
20. Toris CB, Gelfman C, Whitlock A, Sponsel WE, Rowe-Rendleman CL. Making basic science studies in glaucoma more clinically relevant: the need for a consensus. *J Ocul Pharmacol Ther*. 2017;33:501–518.
21. Kuerten D, Fuest M, Koch EC, Remky A, Plange N. Long term effect of trabeculectomy on retrobulbar haemodynamics in glaucoma. *Ophthalmic Physiol Opt*. 2015;35:194–200.
22. Januleviciene I, Siaudvytyte L, Diliene V, Barsauskaite R, Siesky B, Harris A. Effect of trabeculectomy on ocular hemodynamic parameters in pseudoexfoliative and primary open-angle glaucoma patients. *J Glaucoma*. 2015;24:e52–e56.
23. Trible JR, Sergott RC, Spaeth GL, et al. Trabeculectomy is associated with retrobulbar hemodynamic changes. A color Doppler analysis. *Ophthalmology*. 1994;101:340–351.
24. Berisha F, Schmetterer K, Vass C, et al. Effect of trabeculectomy on ocular blood flow. *Br J Ophthalmol*. 2005;89:185–188.
25. Poinoosawmy D, Indar A, Bunce C, Garway-Heath DF, Hitchings RA. Effect of treatment by medicine or surgery on intraocular pressure and pulsatile ocular blood flow in normal-pressure glaucoma. *Graefes Arch Clin Exp Ophthalmol*. 2002;240:721–726.
26. Mackenzie PJ, Cioffi GA. Vascular anatomy of the optic nerve head. *Can J Ophthalmol*. 2008;43:308–312.
27. Hayreh SS. Blood supply of the optic nerve head and its role in optic atrophy, glaucoma, and oedema of the optic disc. *Br J Ophthalmol*. 1969;53:721–748.
28. Lee EJ, Kim TW, Weinreb RN, Kim H. Reversal of lamina cribrosa displacement after intraocular pressure reduction in open-angle glaucoma. *Ophthalmology*. 2013;120:553–559.
29. Zhi Z, Cepurna WO, Johnson EC, Morrison JC, Wang RK. Impact of intraocular pressure on changes of blood flow in the retina, choroid, and optic nerve head in rats investigated by optical microangiography. *Biomed Opt Express*. 2012;3:2220–2233.
30. Best M, Blumenthal M, Galin MA, Toyofuku H. Fluorescein angiography during induced ocular hypertension in glaucoma. *Br J Ophthalmol*. 1972;56:6–12.
31. Lee EJ, Kim TW, Kim M, Kim H. Influence of lamina cribrosa thickness and depth on the rate of progressive retinal nerve fiber layer thinning. *Ophthalmology*. 2015;122:721–729.
32. Furlanetto RL, Park SC, Damle UJ, et al. Posterior displacement of the lamina cribrosa in glaucoma: in vivo interindividual and intereye comparisons. *Invest Ophthalmol Vis Sci*. 2013;54:4836–4842.
33. Yang H, He L, Gardiner SK, et al. Age-related differences in longitudinal structural change by spectral-domain optical coherence tomography in early experimental glaucoma. *Invest Ophthalmol Vis Sci*. 2014;55:6409–6420.
34. Rhodes LA, Huisingh C, Johnstone J, et al. Peripapillary choroidal thickness variation with age and race in normal eyes. *Invest Ophthalmol Vis Sci*. 2015;56:1872–1879.
35. Saeedi O, Pillar A, Jefferys J, Arora K, Friedman D, Quigley H. Change in choroidal thickness and axial length with change in intraocular pressure after trabeculectomy. *Br J Ophthalmol*. 2014;98:976–979.
36. Levitzky M, Henkind P. Angioarchitecture of the optic nerve. II. Lamina cribrosa. *Am J Ophthalmol*. 1969;68:986–996.
37. Tokayer J, Jia Y, Dhalla AH, Huang D. Blood flow velocity quantification using split-spectrum amplitude-decorrelation angiography with optical coherence tomography. *Biomed Opt Express*. 2013;4:1909–1924.
38. Pechauer AD, Jia Y, Liu L, Gao SS, Jiang C, Huang D. Optical coherence tomography angiography of peripapillary retinal blood flow response to hyperoxia. *Invest Ophthalmol Vis Sci*. 2015;56:3287–3291.
39. Huang D, Jia Y, Gao SS, Lumbroso B, Rispoli M. Optical coherence tomography angiography using the Optovue device. *Dev Ophthalmol*. 2016;56:6–12.
40. Jia Y, Morrison JC, Tokayer J, et al. Quantitative OCT angiography of optic nerve head blood flow. *Biomed Opt Express*. 2012;3:3127–3137.
41. Jia Y, Bailey ST, Hwang TS, et al. Quantitative optical coherence tomography angiography of vascular abnormalities in the living human eye. *Proc Natl Acad Sci U S A*. 2015;112:E2395–E2402.
42. Spaide RF, Fujimoto JG, Waheed NK. Image artifacts in optical coherence tomography angiography. *Retina*. 2015;35:2163–2180.
43. Akagi T, Iida Y, Nakanishi H, et al. Microvascular density in glaucomatous eyes with hemifield visual field defects: an optical coherence tomography angiography study. *Am J Ophthalmol*. 2016;168:237–249.

Investigative Ophthalmology & Visual Science